Dynamic Load Distribution in Continuous I-Beam Highway Bridges

D. A. LINGER, Associate Professor of Civil Engineering, University of Arizona, and
C. L. HULSBOS, Research Professor of Civil Engineering, Lehigh University

The load distribution to the longitudinal beams is shown for the outer and inner spans and at the interior supports for two types of continuous four-span highway bridges. The load distribution was determined for static and moving loads and indicates the effect of dynamic loading on lateral load distribution. The effective composite sections were determined experimentally for the negative as well as the positive moment regions.

From the results of the load distribution data, influence lines are presented for the lateral distribution of loads and a comparison is made with the AASHO specifications. The effective composite section of the longitudinal stringers, which was required for the load distribution study, is shown and indicates that the distribution and amount of composite action vary from that allowed by the AASHO specifications.

•THE PROBLEM of load distribution in highway bridges made up of longitudinal stringers acting integrally with a roadway slab has been investigated by many researchers (1, 2, 3, 4, 5, 6, 7, 8). These investigations have added materially to the knowledge of the response of highway bridges to vehicular loading. However, the expanded use of this type of bridge has emphasized the need for a better understanding of the way in which it responds to dynamic vehicular loading. Moreover, it is quite evident that the problem of load distribution is not just a static problem, but a dynamic problem. It is this dynamic problem that has been generally ignored by highway engineers and is becoming increasingly important as larger and faster vehicles are used.

The research presented herein is a summary of a load distribution study conducted by the authors in conjunction with a research project (4, 5). To present and discuss the additional data obtained in the experimental program for the impact study, the following report on static and dynamic load distribution and the effective section of the longitudinal stringers is presented.

The investigation of dynamic load distribution was made by first studying how the static live load is distributed to the stringers by the distribution of the bending moments. After the static load distribution was obtained, the dynamic effect of the moving load was studied for its effect on the whole bridge as well as on the individual stringers. The load distribution studies also indicate that considerable longitudinal load distribution occurs in the type of structures studied. The effective section of the longitudinal stringers was required for these studies, and the results of this experimental data add to the understanding of the complex problem of the amount of composite action in a continuous highway bridge.

OBJECTIVE

The objective of this research was to evaluate the response of full-size continuous I-beam highway bridges to dynamic vehicle loadings. The objective of the portion of

Paper sponsored by Committee on Bridges.

the research presented herein was to analyze the effect of dynamic loads on lateral live-load distribution and to present the influence lines for the lateral live-load distribution for the various longitudinal stringers. An additional objective, which is basic to the design of this type of structure, was to determine the amount of effective composite action between the reinforced concrete slab and the longitudinal stringers.

BRIDGE STRUCTURES

The bridges tested are part of the Interstate Highway System around Des Moines, Iowa. Only two of the four bridges studied in this research program are reported in this paper. The two bridge structures included are a continuous aluminum stringer bridge, and a continuous steel stringer bridge (5). Both bridges carry two lanes of traffic and were designed for an H20-S16 loading.

Continuous Aluminum Stringer Bridge

This structure is a 220-ft continuous four-span bridge with four aluminum stringers which act compositely with a reinforced concrete roadway. It has a 30-ft roadway with a 3-ft safety curb on both sides (Fig. 1). It carries traffic on Clive Road over Interstate 35 northwest of Des Moines.

Continuous Steel Stringer Bridge

This 240-ft continuous four-span structure is very similar to the previous bridge except for the longitudinal stringers. The four steel stringers act compositely with a reinforced concrete roadway which is 28 ft wide with a 3-ft safety curb on both sides (Fig. 2). This structure carries the traffic on Ashworth Road over Interstate 35 west of Des Moines.

VEHICULAR LOADING

The vehicle used in the experimental study is a tandem-axle, International L-190 van type truck (Fig. 3). This truck, which is used to check the Iowa State Highway

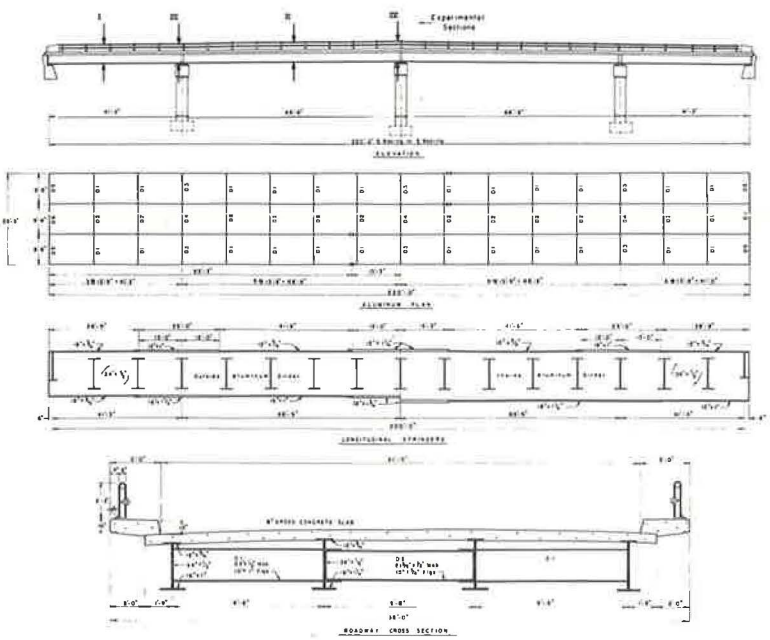

Figure 1. Details of continuous aluminum stringer bridge.

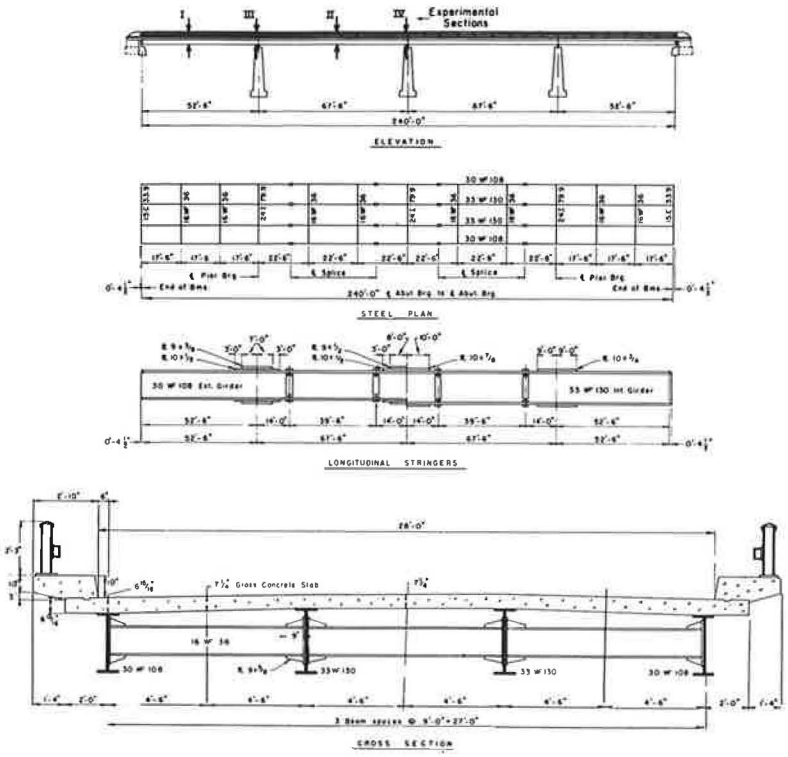

Figure 2. Details of continuous steel WF stringer bridge.

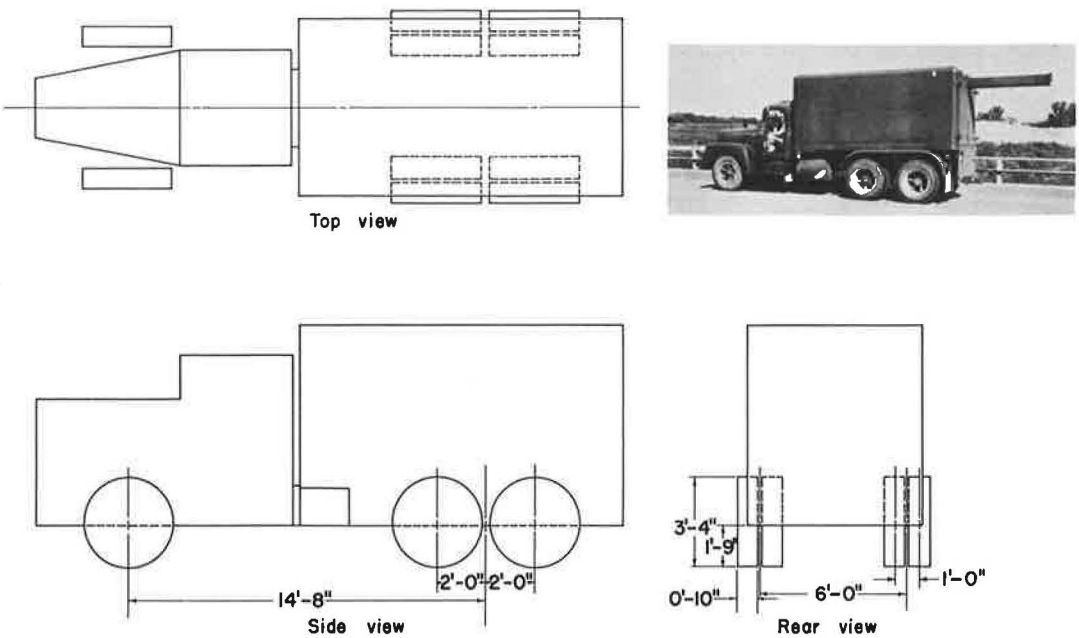

Figure 3. The standard (H-20) loading vehicle.

Commission scales, has a wheel base of 14 ft, 8 in. and a tread of 6 ft. It weighs 40,650 lb with 21,860 lb on the rear axle. This vehicle closely approximates a standard H-20 design load.

The static load distribution was determined by the test vehicle creeping across the bridge with the motor idling. This loading was applied on all the experimental test "lanes" of the bridges (Figs. 4 and 5). Each of the experimental lanes was marked by a painted stripe along which the left front tire of the truck was run. During the speed runs which were used to evaluate the dynamic load distribution, the variation of the position of the vehicle to one side or the other was never more than 1½ in. The dynamic tests were performed along four different lanes on the bridge roadway, two lanes for each direction of travel with one lane corresponding to the highway lane and the other lane at the longitudinal center line of the bridge.

INSTRUMENTATION

Strain Recording Equipment

To determine the dynamic effect of the vehicles, the static and dynamic bridge moments were computed from the strain measured at the extreme bottom fiber of each stringer. To measure the strains, standard SR-4 strain gauges were used.

The strain readings were recorded by a Brush universal amplifier (BL-520) and a Brush direct-writing recorder (BL-274). This equipment produces a continuous record of strain for which the time base can be varied by the speed of the recording paper.

Location of Strain Gauges

The strains were measured in all the stringers in the outer and inner spans and at the interior supports. This allowed the load distribution to be evaluated at all the sections of maximum bending moment for the entire length of the bridge structures. The distribution of live load and the effect of dynamic loading were determined for negative as well as positive moment sections.

Experimental Sections.—The experimental sections instrumented for the evaluation of the bridge moments are described in the following and shown in Figures 1 and 2.

(1) Section 1 is located at a point four-tenths of the outer span from the end support.
(2) Section 2 is located at the middle of the interior span.
(3) Section 3 is located at the first interior support. To eliminate or reduce any effect which the reaction diaphragms might have, section 3 was offset from the center

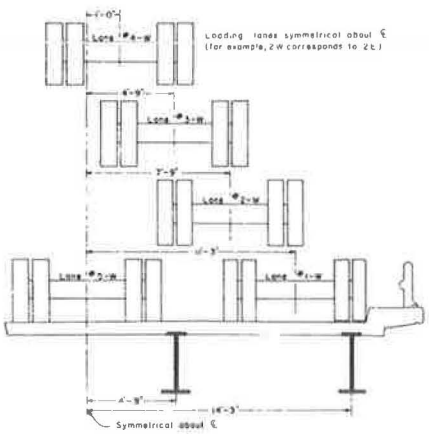

Figure 4. Cross-section showing test "lanes" for the aluminum stringer bridge.

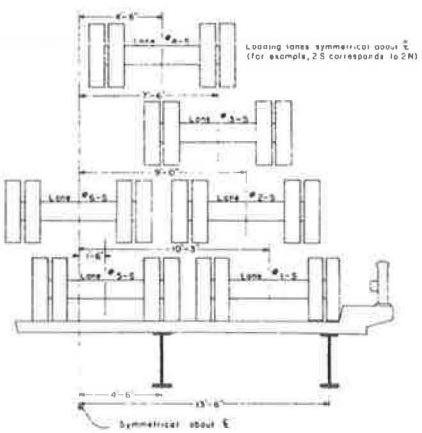

Figure 5. Cross-section showing test "lanes" for the steel stringer bridge.

line of the reaction toward the exterior span. This offset was 1 ft for the aluminum stringer, and 6 in. for the steel stringer bridge.

(4) Section 4 is located at the center interior support. This section is offset from the center line of the reaction a distance equal to the offset of section 3 for each respective bridge structure.

All of the bridges were instrumented at each of the above sections with an SR-4 strain gauge at the center of the bottom flange.

Experimental Neutral Axes.—To obtain the moments required to evaluate the distribution of load, the section moduli of the stringers were required at the sections where the strains were measured. The effective composite section of the longitudinal stringers varies considerably due to cover plates, variable flanges or the proximity of the curb to the outer stringers. These variations in the cross-section result in large changes in the moments of inertia and section moduli from one section to another. The actual section moduli and moments of inertia of the longitudinal stringers were determined experimentally by obtaining the position of the neutral axis of the longitudinal stringers. Five SR-4 strain gauges were positioned at each cross-section of the stringer for which the location of the neutral axis was required. One gauge was located at the center of gravity of the longitudinal stringer, and the other four gauges were at the extreme fibers and the quarter points. The locations of the neutral axes were then determined by plotting to scale the strains obtained from the gauges along each cross-section for various static loadings on the bridge. The neutral axis could then be located very accurately to the nearest $\frac{1}{8}$ in. Once the neutral axes were obtained, the amount of slab necessary to balance the experimentally located neutral axes was determined and the moments of inertia computed. The entire roadway slab thickness was used in these calculations with a modular ratio of 10 for the steel stringer bridge and a ratio of 3.33 for the aluminum stringer bridge. However, once the position of the neutral axis is known, the moment of inertia is independent of the modular ratio used.

TEST RESULTS

The Composite Section

The neutral axes of the stringer cross-sections were determined at the four experimental sections (Figs. 1 and 2) for the aluminum and steel stringer bridges. Only one quadrant of each bridge was instrumented to determine the position of the neutral axes because the bridges are symmetrical about their lateral and longitudinal center lines. The cross-sections of the aluminum and steel stringer bridges at sections 1, 2, 3, and 4 are shown in Figures 6 and 7.

The neutral axes results are not intended for a complete analysis of the variations in cross-section along the entire length of the bridges. They do show that the actual composite cross-section varies greatly at different sections along the bridges as indicated in previous research (3).

Aluminum Stringer Bridge.—The present AASHO specifications would allow 96.0 in. of slab to be used with the interior stringers and 62.25 and 69.0 in. to be used with the exterior stringers in the outer and inner spans, respectively. The experimental results indicate that there is more slab acting compositely than the specifications would allow, except at the interior stringer at section 1. This section of the interior stringer used 3 in. of slab less than that allowed by the specifications. In both positive moment sections, the resulting exterior composite sections are approximately 17 percent less than their corresponding interior composite sections even though the aluminum sections used in the exterior beams were considerably smaller. It is evident from Figure 6 that both the interior and exterior stringers exhibit considerable composite action at sections 3 and 4. This negative moment region would not be allowed composite action according to the specifications.

Steel Stringer Bridge.—The AASHO specifications would allow 87.0 and 67.5 in. of slab to be used with the interior and exterior stringers in all spans. The experimental slab width acting compositely with the interior stringer, is approximately 85 percent of the slab width allowed by the AASHO specifications. Conversely, the experimental

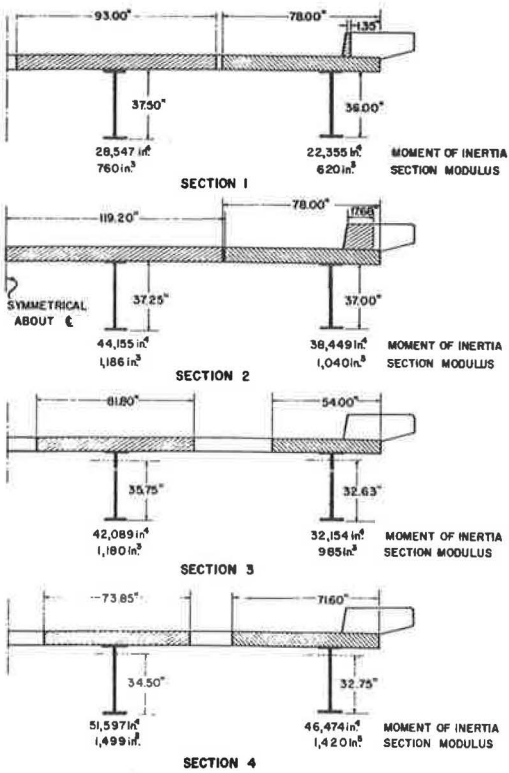

Figure 6. A cross-section of the aluminum stringer bridge at sections 1, 2, 3, and 4 showing the composite moments of inertia, section moduli, and the effective slab.

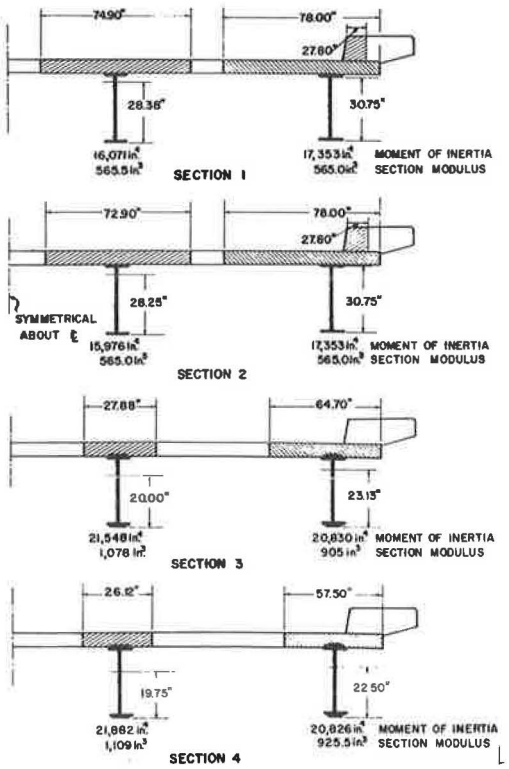

Figure 7. A cross-section of the steel stringer bridge at sections 1, 2, 3, and 4 showing the composite moments of inertia, section moduli, and the effective slab.

slab width acting compositely with the exterior stringer is considerably greater than the amount allowed by the AASHO specifications (Fig. 7). The exact amount of slab is questionable because the sidewalk curb acts integrally with the slab and must be considered in the composite action. It was decided arbitrarily that if more slab was necessary than available, the acting width of slab would be limited to the distance from the slab edge to the mid-point between the stringers, and the remaining amount of concrete necessary to balance the experimental neutral axis would be obtained from the sidewalk curb. This approach was used for both the aluminum and the steel stringer bridges. The reduction in the composite action of the interior stringers over that allowed by the specifications is more than offset by the increase in composite action of the exterior stringers. This increase in composite action at the exterior stringer is more evident in the steel stringer bridge than in the aluminum stringer bridge. The individual composite moments of inertia of the steel stringers are within four percent of their average, whereas the interior and exterior composite sections specified by AASHO are considerably different. The similarity of the actual experimental composite moments of inertia is also evident at experimental sections 3 and 4 which are in negative moment regions. The specifications do not allow any composite action to be used in these regions even though considerable composite action was found.

The composite action occurring in the negative moment regions of the aluminum and steel stringer bridges may be partially due to the way in which the continuous bridges are constructed in Iowa. The roadway slab of this type bridge is placed first in the positive moment sections and then in the negative moment portion of the roadway. As a result, the dead-load tensile stresses in the slab at the supports are minimized.

Also, the shear connectors are extended over the entire length of the stringers, and in some cases, additional reinforcement is placed in the slab over the bridge piers.

Load Distribution

Static Live Load.—The distribution of load in a slab stringer bridge is not readily analyzed by an exact method. Several theoretical methods which offer a convenient means of determining the amount of the live load distributed to each longitudinal stringer have been proposed (1, 2, 6). This report includes only the presentation of data and does not attempt to correlate the data with any theoretical results.

In this experimental study, the load distribution was determined by using the individual moment in each stringer as a percent of the total moment in the bridge cross-section. This procedure gives the percentage of the total live load distributed into each stringer, providing the moment diagrams for all the stringers are identical in shape. This is the assumption used in the design of this type of bridge structure. The live-load moments in the stringers were obtained by multiplying the measured live-load strains by the modulus of elasticity of the stringers and the section moduli for the composite cross-sections. The resulting percentage live-load distribution for the aluminum and steel stringer bridges is shown in Figures 8 through 15. This percentage distribution of load does not take into account the longitudinal load distribution because it is only a percent of the total moment. It has been found in previous studies that the experimental moment is considerably less than the theoretical moment which assumes no longitudinal load distribution (3, p. 34).

The static load distribution diagrams, which show little variation from section to section, have been further analyzed. The resulting influence diagrams are discussed later. The form of the influence line lends itself to a direct discussion and application of these results.

Dynamic Load Distribution.—The dynamic response of the bridges tested was obtained by moving-load tests. These moving-load tests were performed on four test

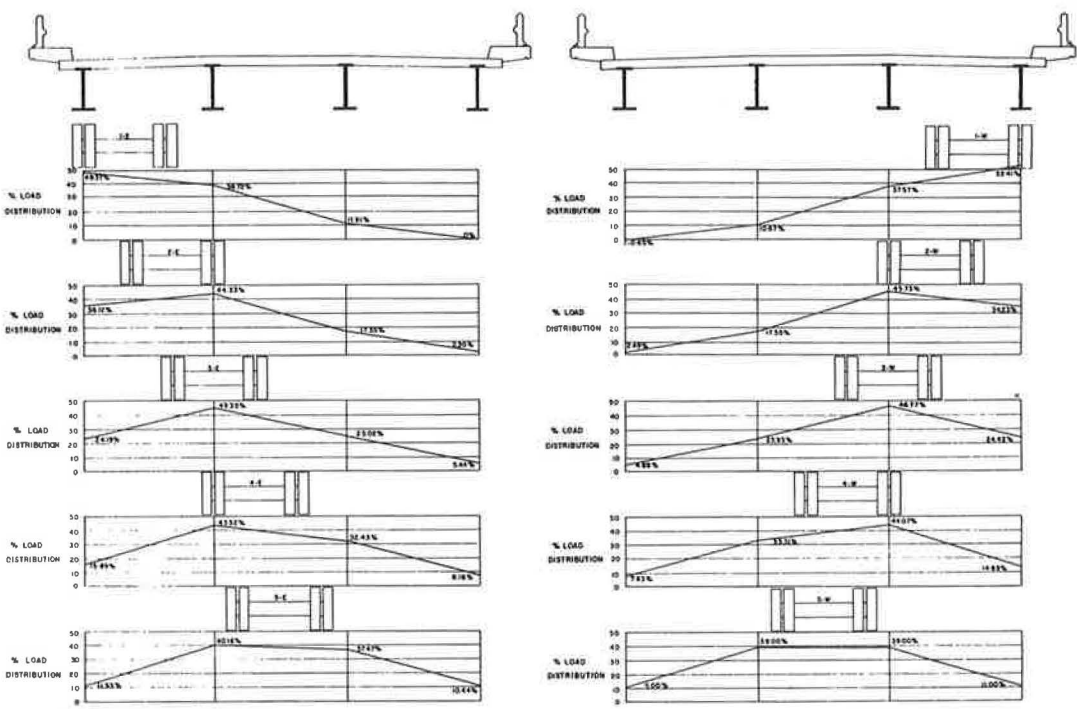

Figure 8. Static load distribution for aluminum stringer bridge at section 1.

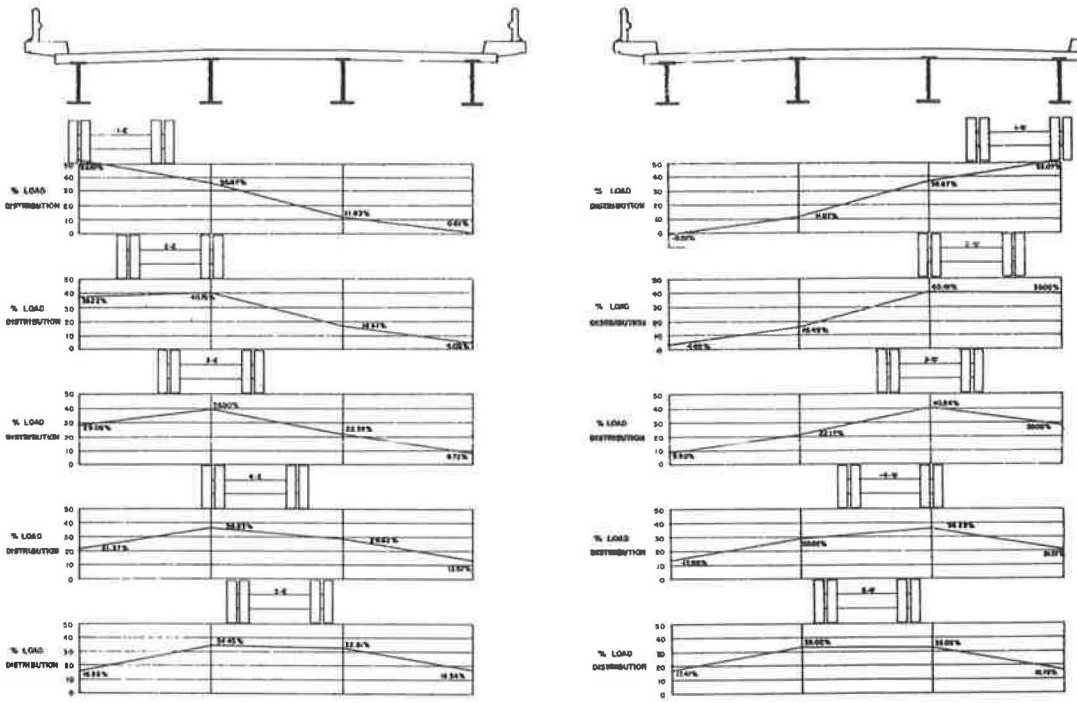

Figure 9. Static load distribution for aluminum stringer bridge at section 2.

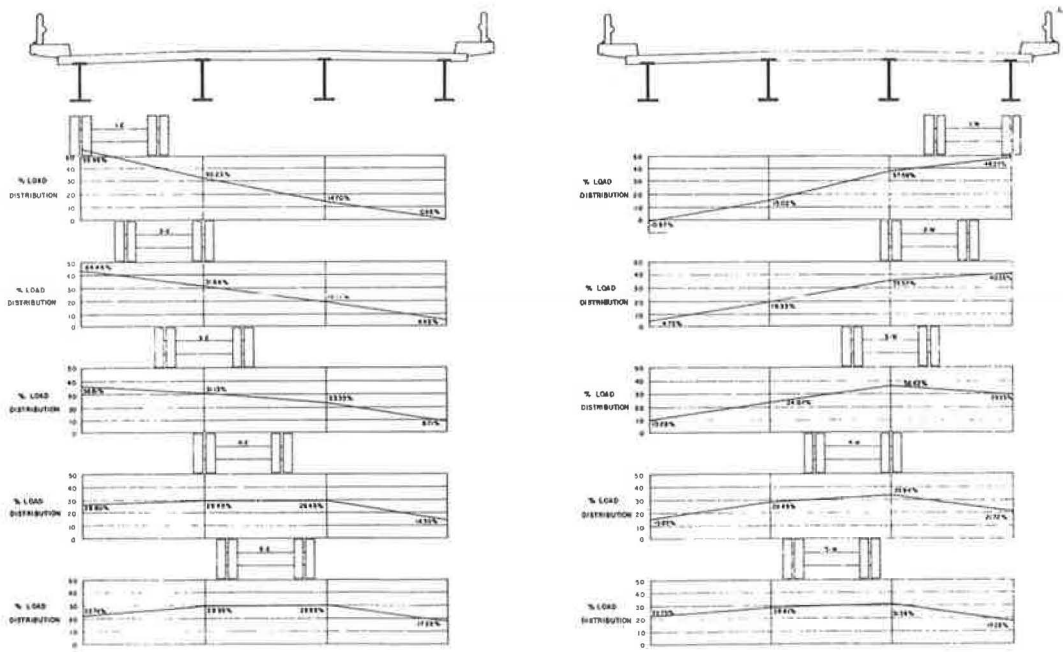

Figure 10. Static load distribution for aluminum stringer bridge at section 3.

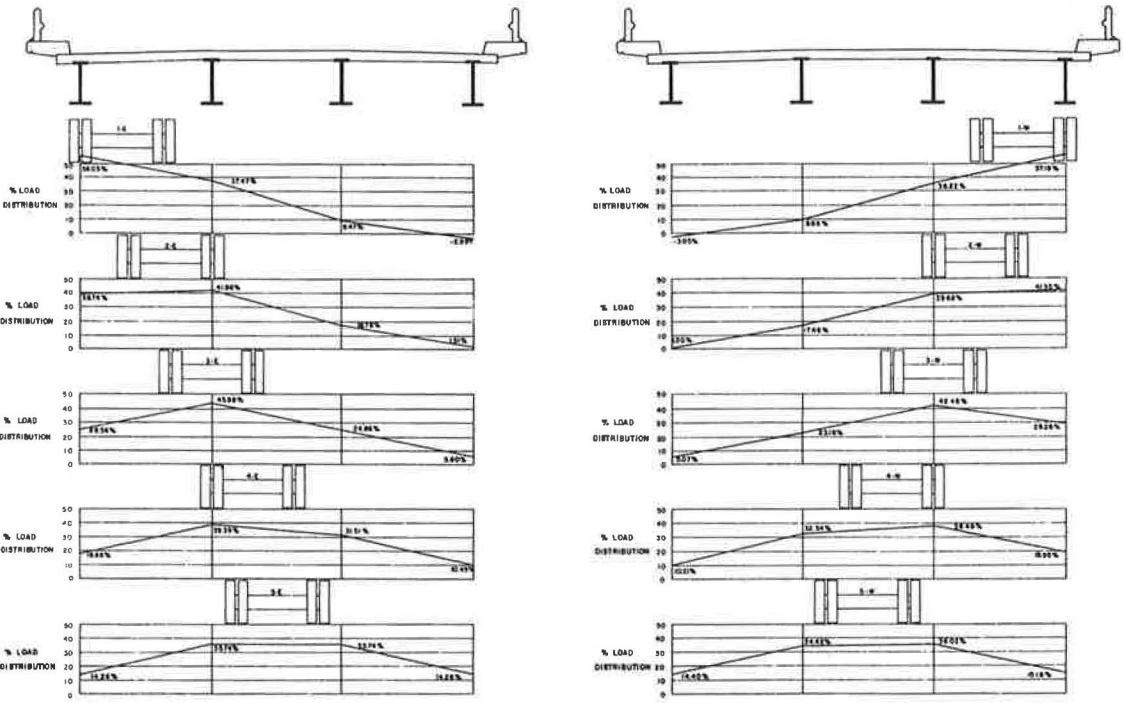

Figure 11. Static load distribution for aluminum stringer bridge at section 4.

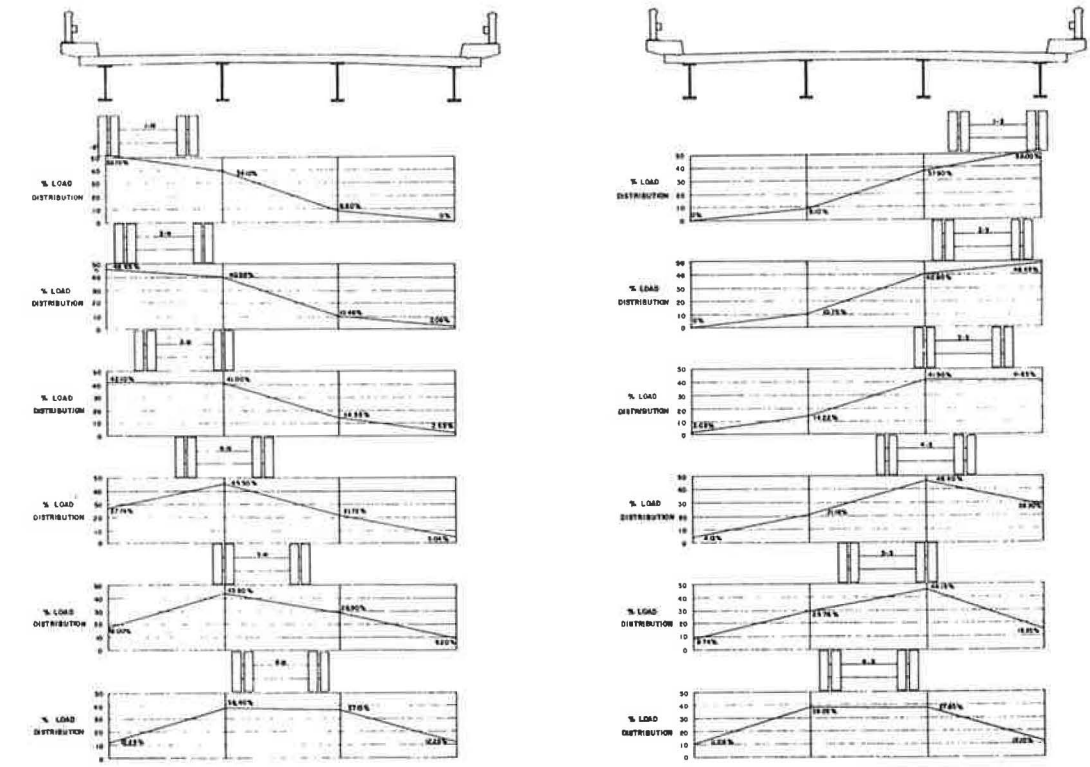

Figure 12. Static load distribution for steel stringer bridge at section 1.

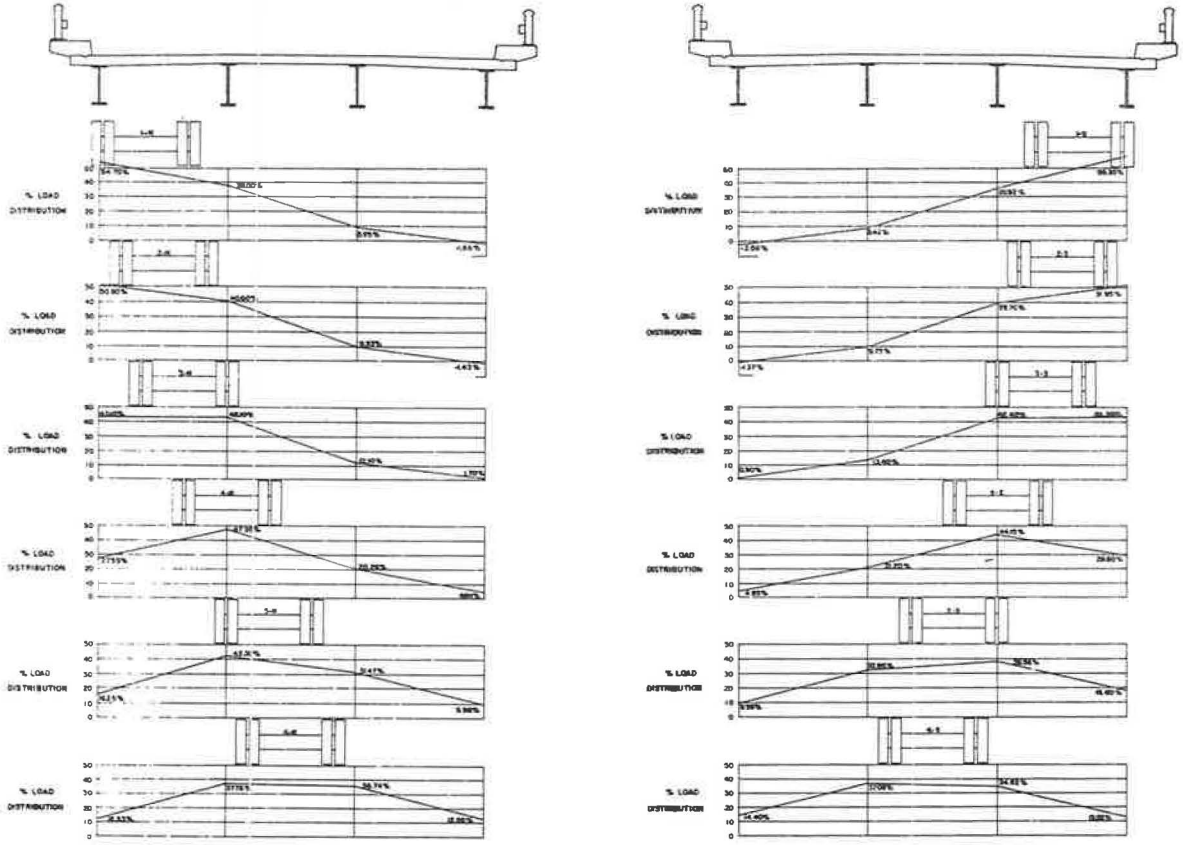

Figure 13. Static load distribution for steel stringer bridge at section 2.

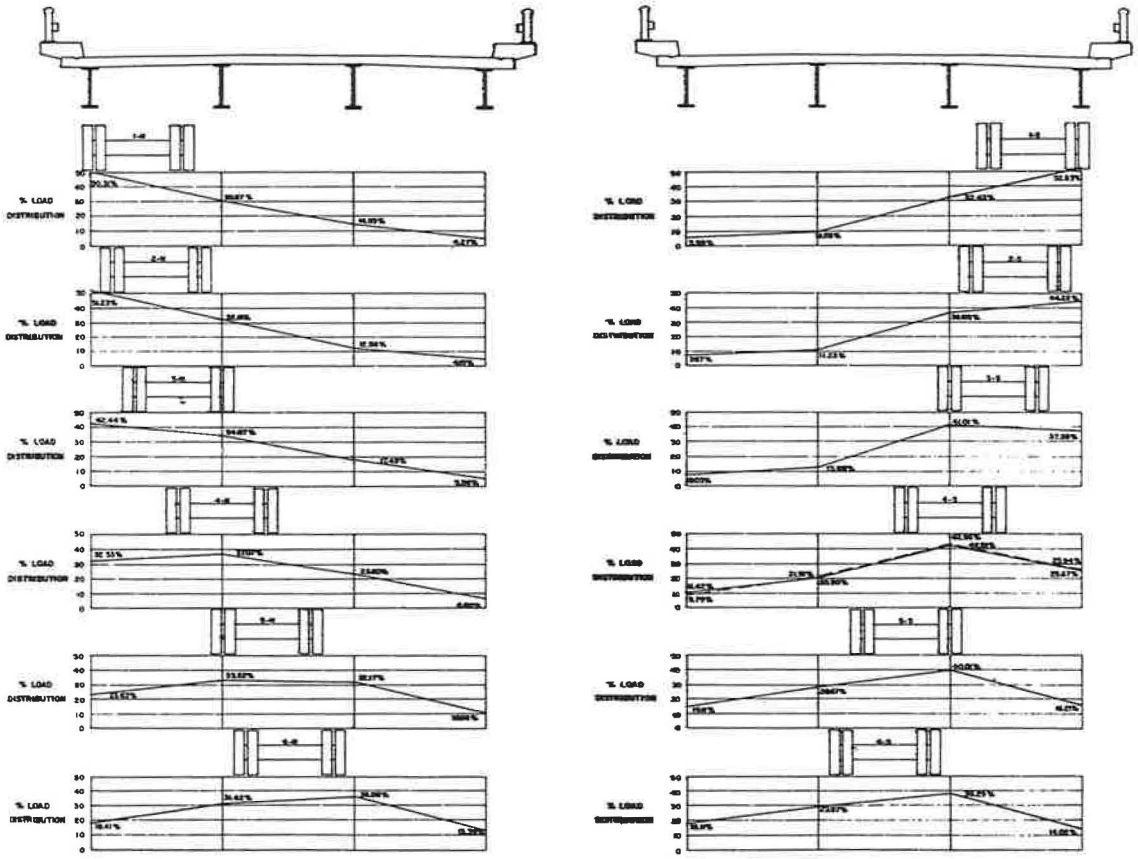

Figure 14. Static load distribution for steel stringer bridge at section 3.

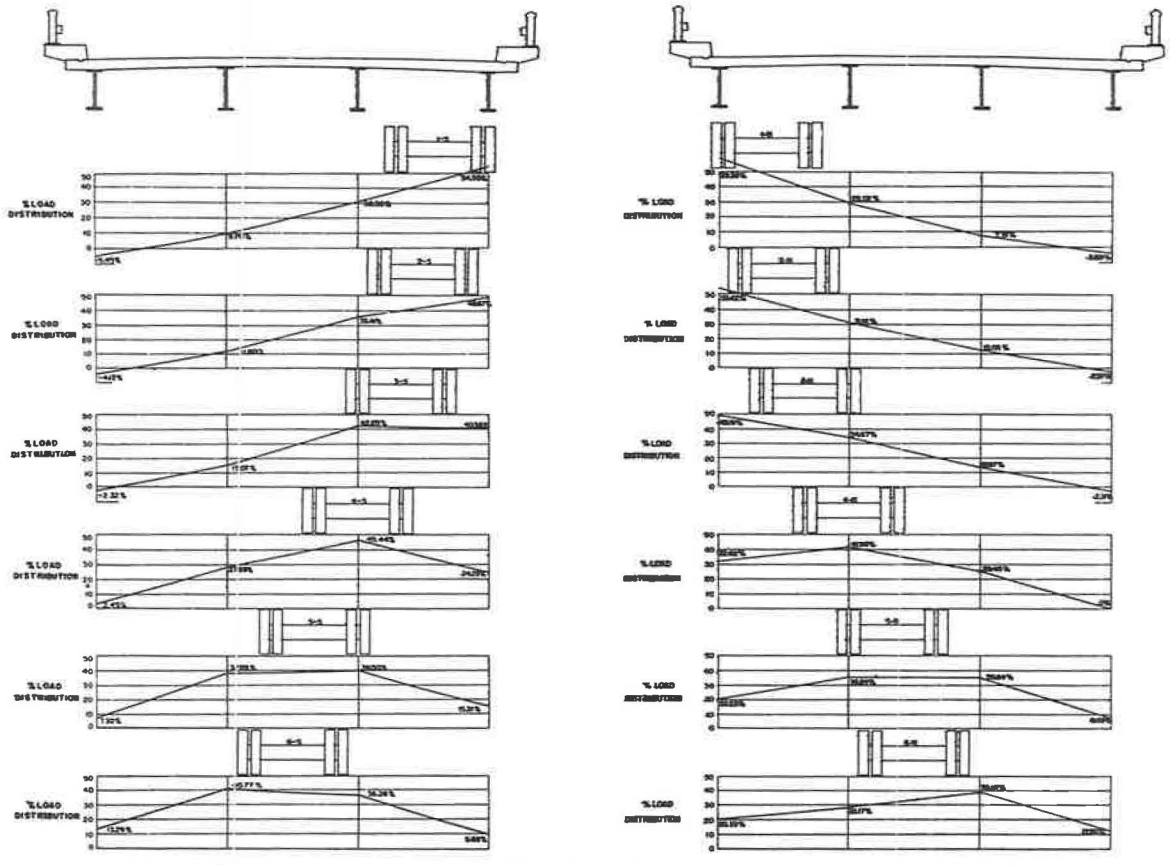

Figure 15. Static load distribution for steel stringer bridge at section 4.

lanes, two for each direction of travel for vehicle speeds beginning at approximately 10 mph and increasing by increments up to the maximum attainable speed. The data from the continuous strain time records were reduced with the vehicle in the same longitudinal position that yielded the maximum static moment.

From these data, the dynamic load distribution to the longitudinal stringers was determined (Figs. 16-23). The dynamic load distribution results indicate a similarity between the static and dynamic load distribution. The largest discrepancies between the static and dynamic load distributions usually occurred at the lower speeds (Figs. 16-23). The largest variation that occurred is eight percent of the load, and the average variation is approximately two and one-half percent of the load. The percentage distribution of moments does not indicate the impact because the percent load distribution is obtained on the basis of the total experimental moment at the section.

The similarity between the static and the dynamic load distribution curves indicates that the vibratory motion of the bridge is superimposed on the static live-load deflection curve for the longitudinal stringers on the other side of the bridge, as well as those under the vehicle. Consequently, the vibration of the bridge did not alter the lateral load distribution to any extent. The largest variation in the lateral load distribution for a dynamic load could have resulted from the lateral "rocking" of the vehicle due to wind and pavement irregularities. However, even this did not materially affect the load distribution. Therefore, the following influence lines for lateral load distribution, although constructed from the static load distribution data, are applicable to dynamic loads as well as static loads.

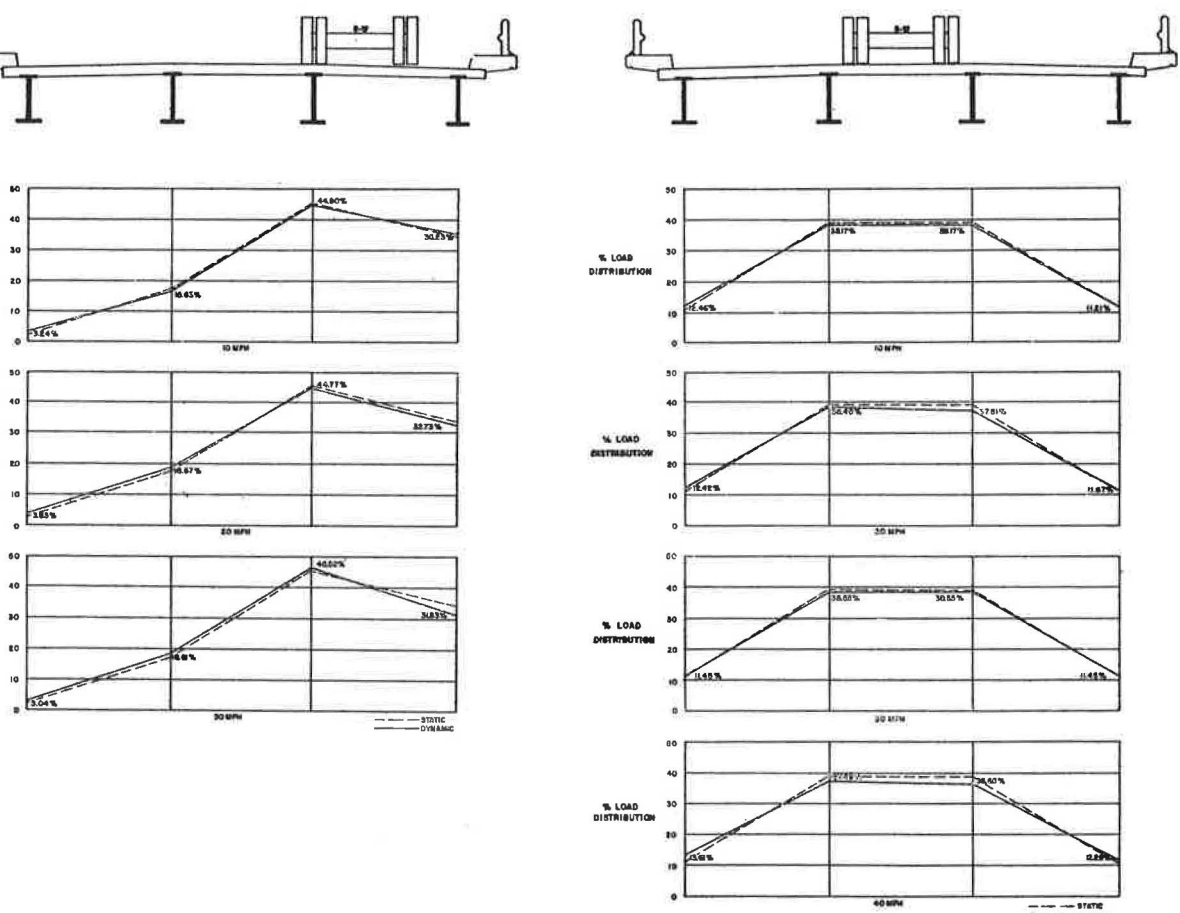

Figure 16. Dynamic load distribution for the aluminum stringer bridge at section 1.

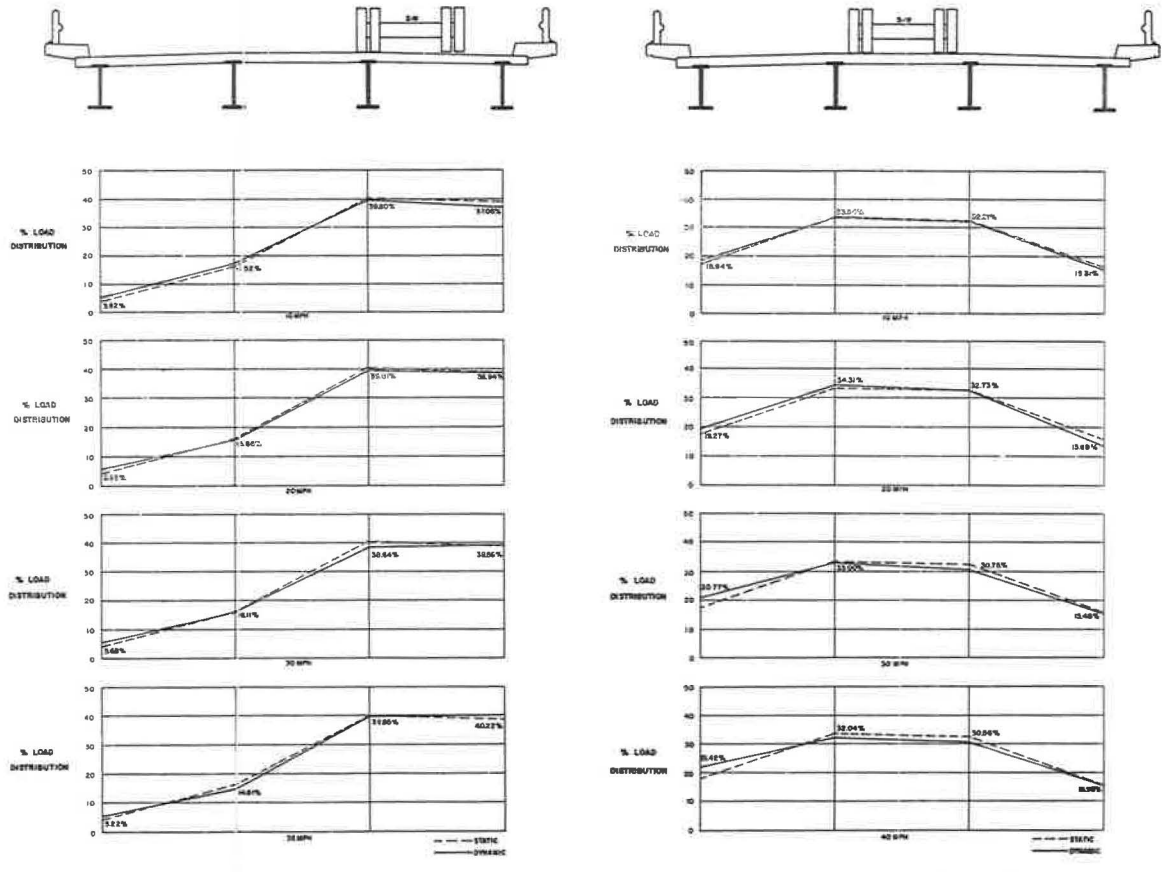

Figure 17. Dynamic load distribution for the aluminum stringer bridge at section 2.

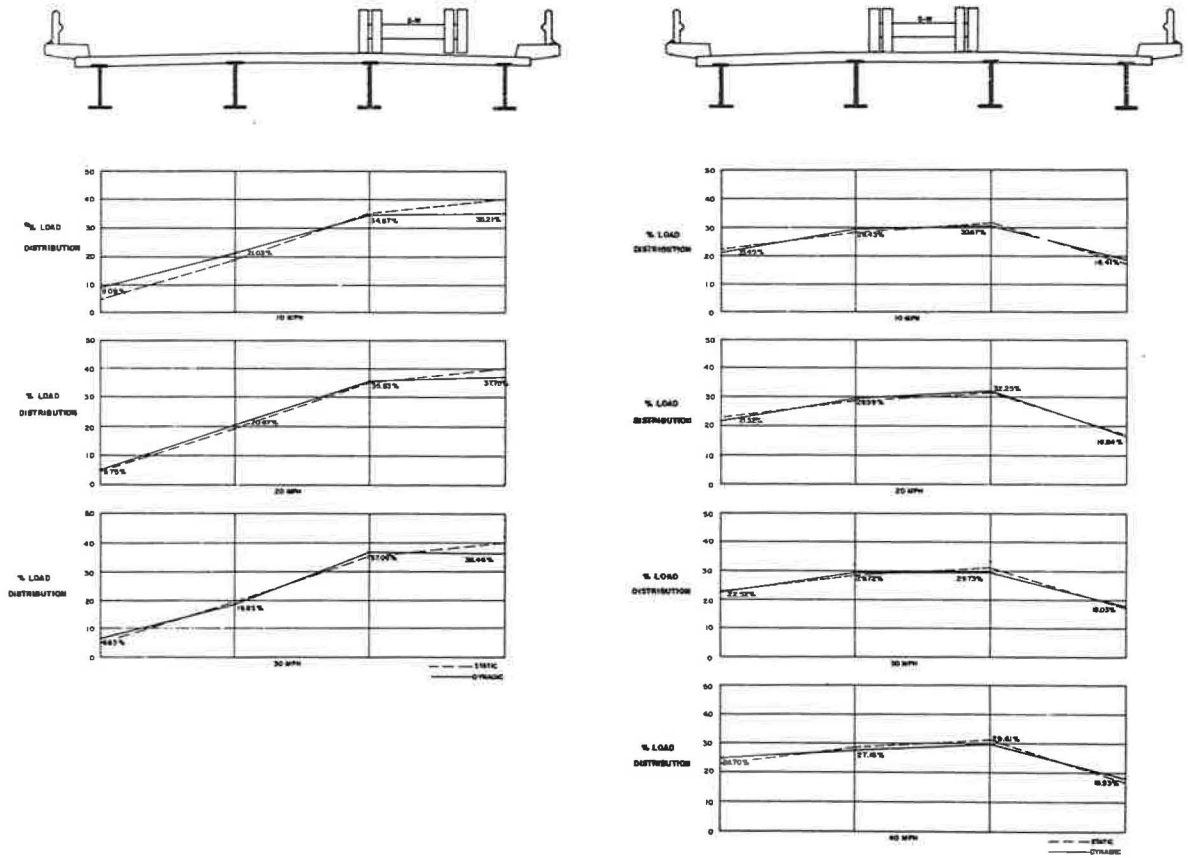

Figure 18. Dynamic load distribution for the aluminum stringer bridge at section 3.

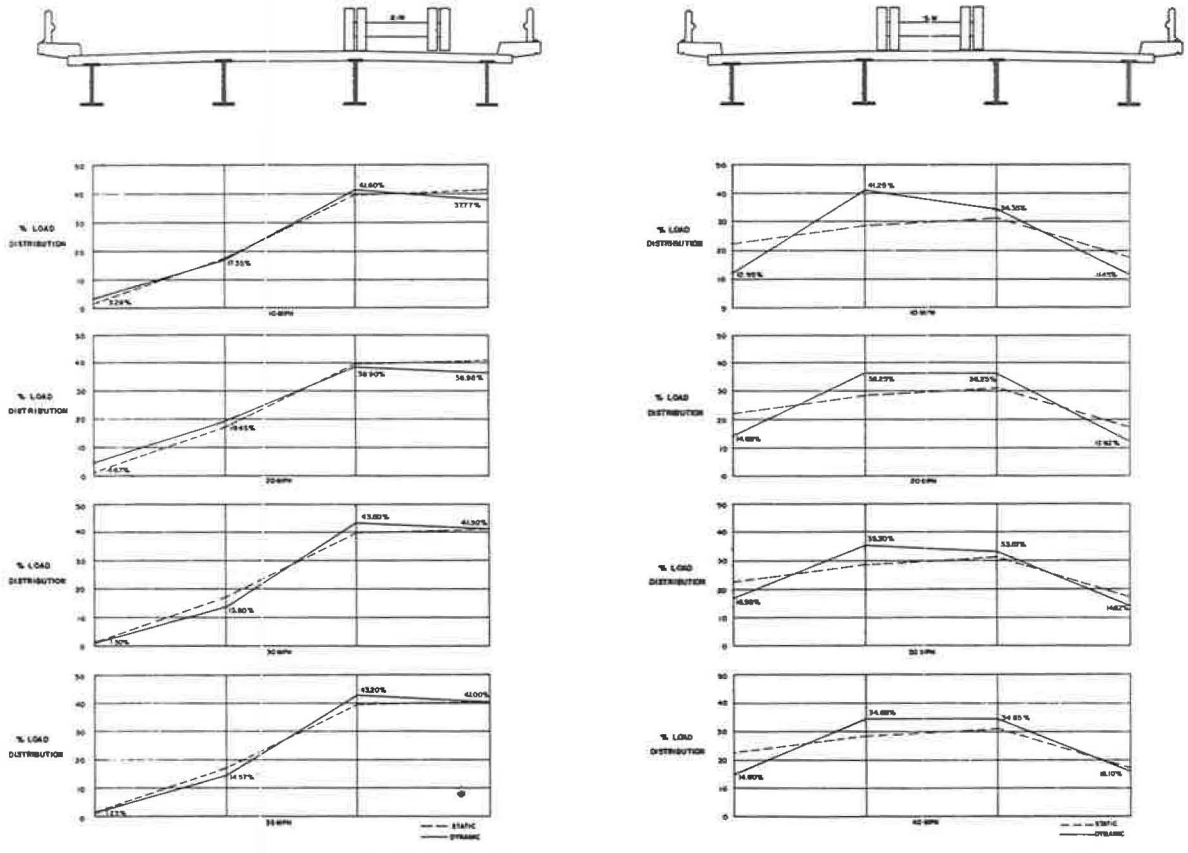

Figure 19. Dynamic load distribution for the aluminum stringer bridge at section 4.

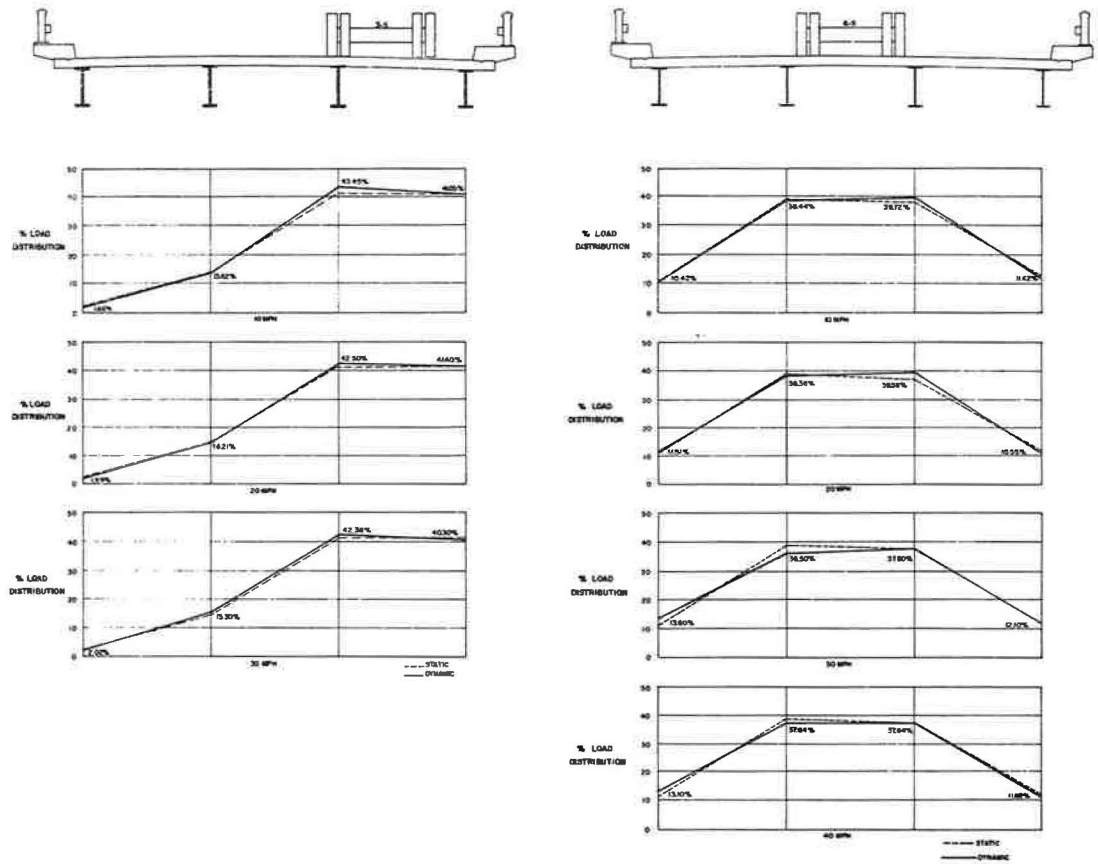

Figure 20. Dynamic load distribution for the steel stringer bridge at section 1.

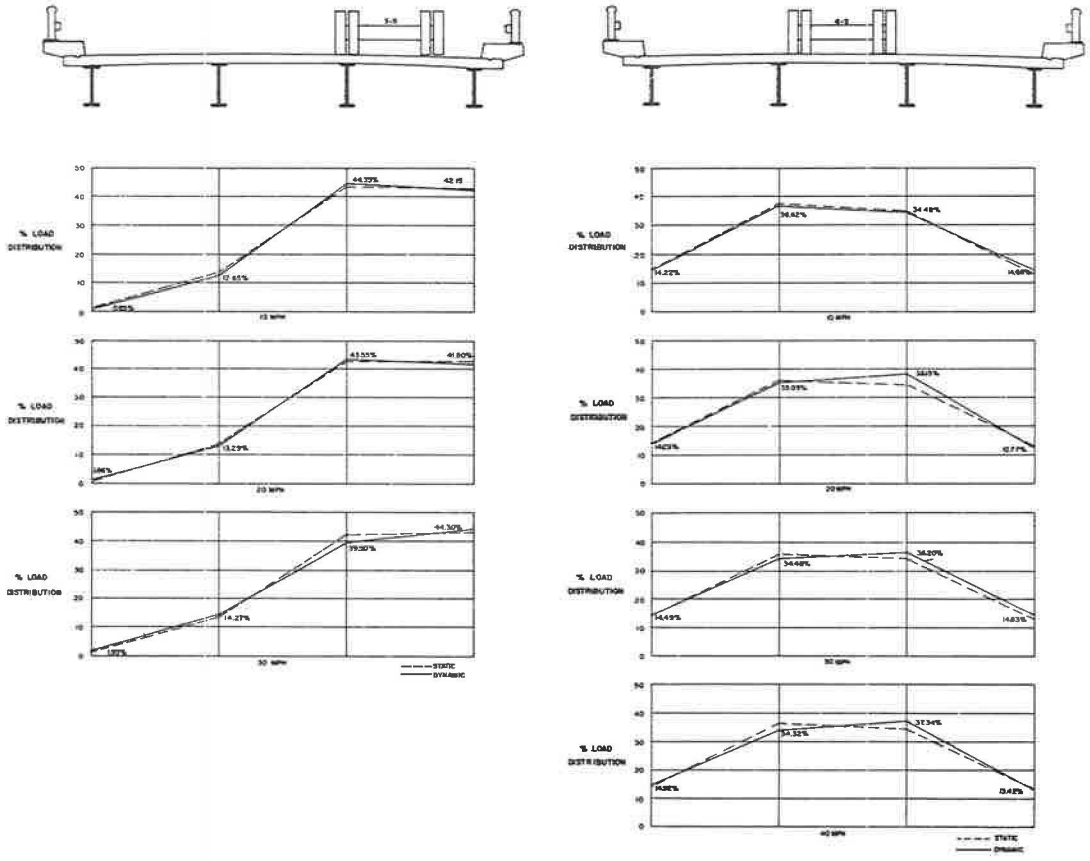

Figure 21. Dynamic load distribution for the steel stringer bridge at section 2.

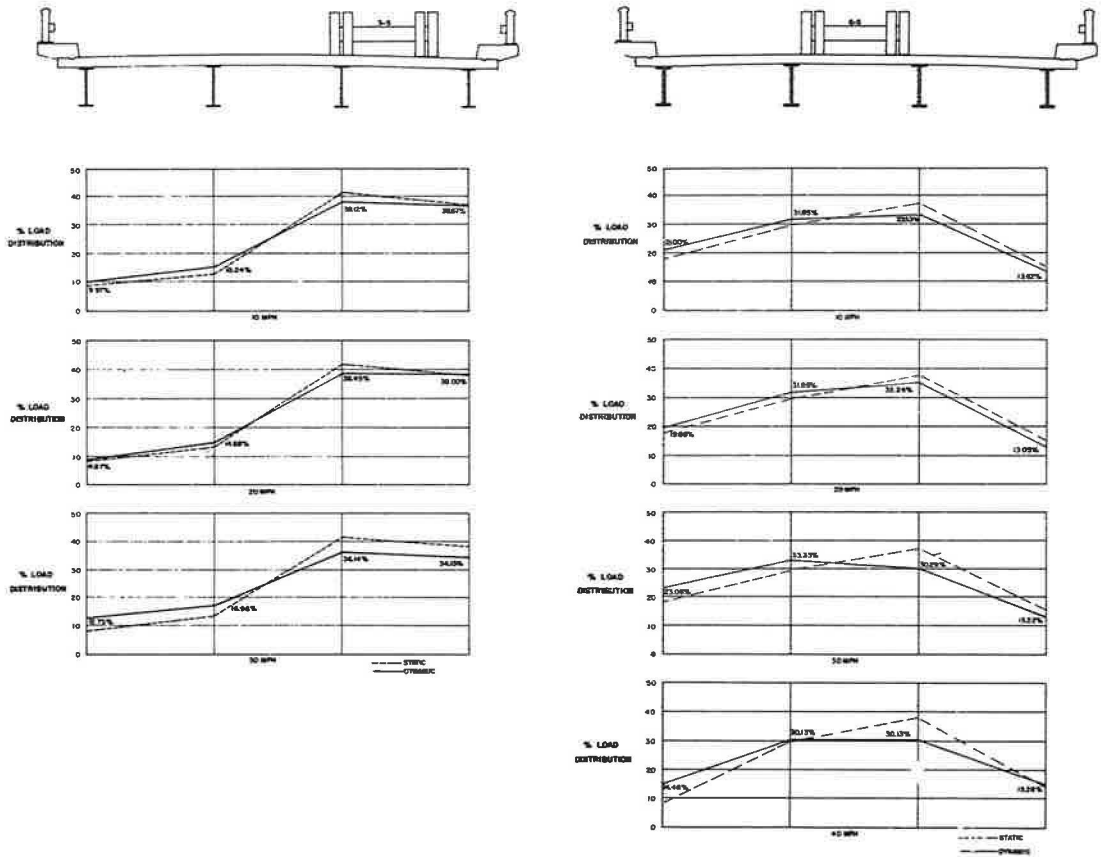

Figure 22. Dynamic load distribution for the steel stringer bridge at section 3.

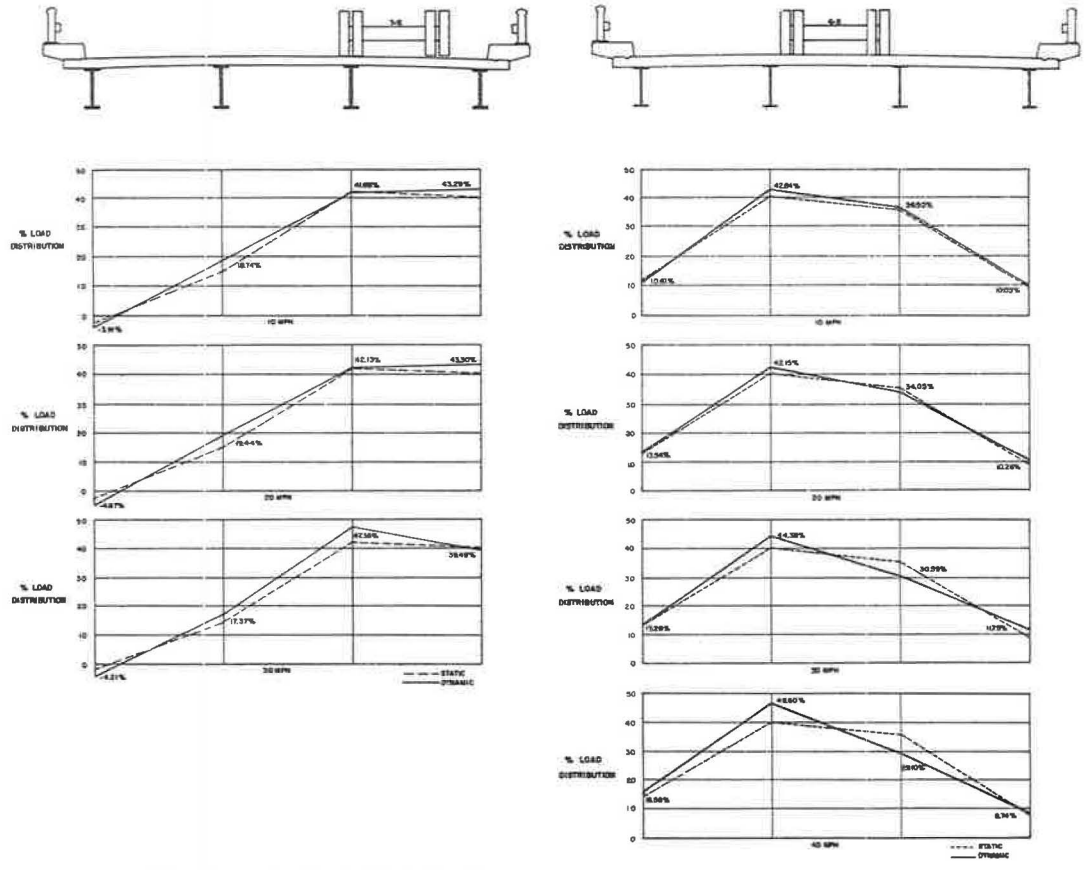

Figure 23. Dynamic load distribution for the steel stringer bridge at section 4.

Influence Lines For The Stringers.—The use of load distribution curves is facilitated by the construction of influence lines for the percentage of a unit vehicle distributed to each stringer. To obtain these influence lines, the static load distribution values were averaged for the symmetrical stringers which correspond with the loading of symmetrical lanes. For example, the value from the one outside stringer with the load in lane 2-S is averaged with the value from the other outside stringer with the load in lane 2-N. These average values were then plotted to correspond with the center line of the vehicle. The resulting influence lines (Figs. 24 and 25) indicate the percentage of a unit vehicle distributed to each respective stringer by the ordinate corresponding to the center line of the vehicle. In order to use these influence lines, it is only necessary to place the desired number of standard vehicles on the bridge cross-section and sum the cumulative influence of each.

Aluminum Bridge Structure.—When two vehicles are placed in their specified lanes and the influence lines in Figure 24 are used, a maximum value of approximately 53 and 57 percent of a vehicle is found to be distributed to an exterior stringer at the positive and negative moment sections, respectively. These percentages of a unit vehicle are equivalent to a wheel-load factor of 1.06 and 1.14, whereas the AASHO specifications yield a wheel-load factor of 1.49 for the exterior stringers in this bridge. Similarly, the maximum percentage of a unit vehicle distributed to an interior stringer at the positive and negative moment sections is approximately 70 and 67 percent, respectively. The equivalent experimental wheel-load factors for these percentages are 1.40 and 1.34, whereas the wheel-load factor given by the AASHO specifications for an interior stringer of this bridge is 1.728. It is interesting to note that the maximum

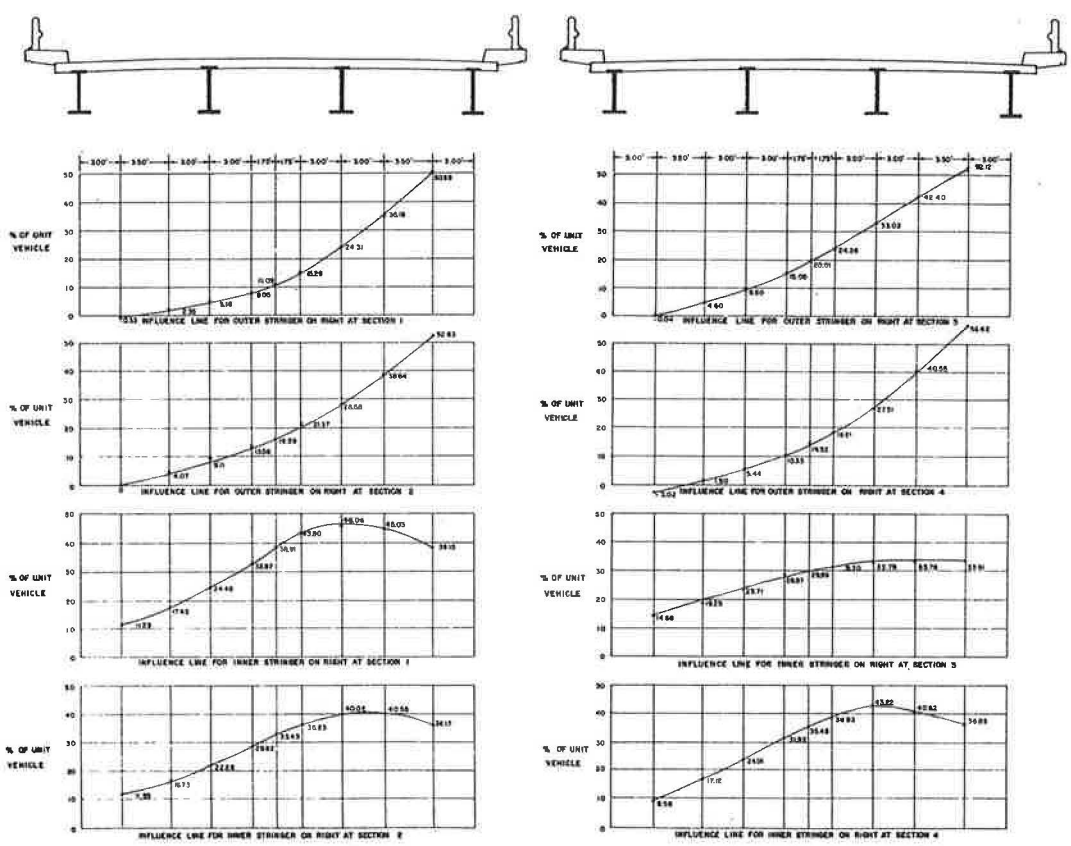

Figure 24. Influence lines for aluminum stringer bridge.

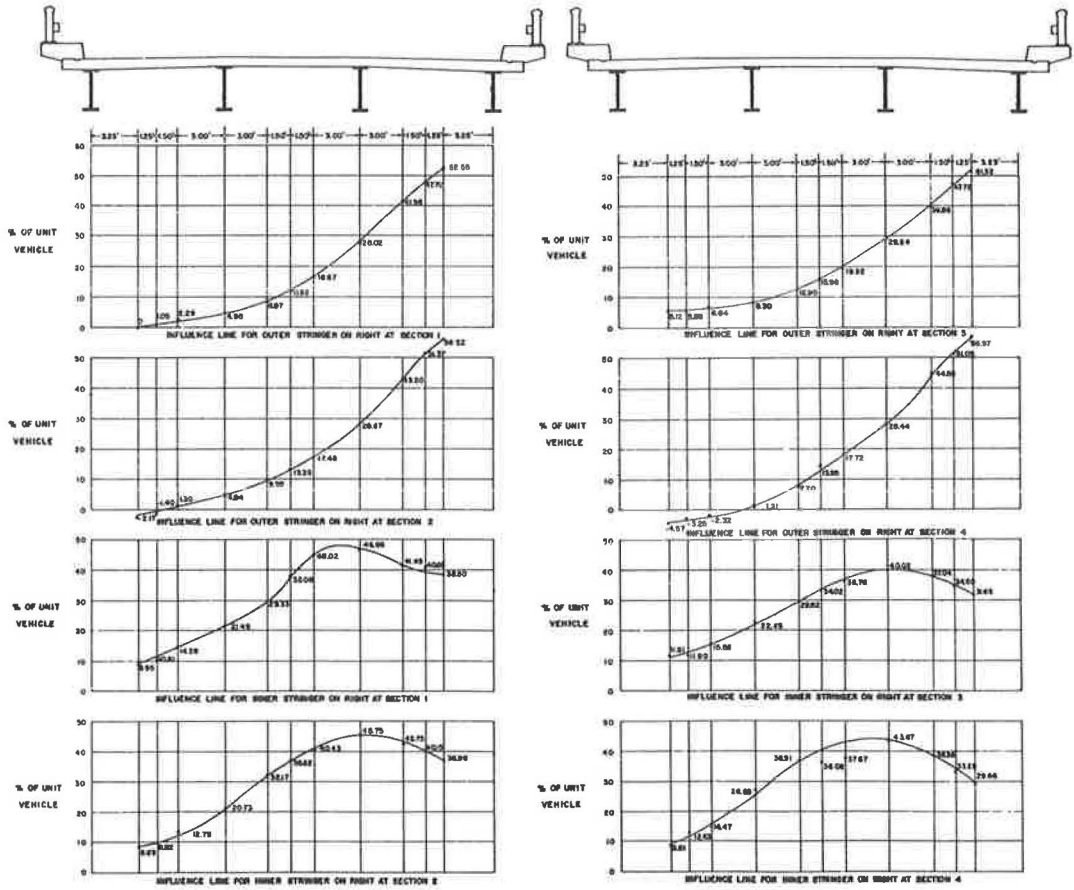

Figure 25. Influence lines for steel stringer bridge.

experimental wheel-load distribution factors occurred at sections 2 and 3 for an exterior stringer and at sections 1 and 4 for interior stringers. The largest wheel-load factors for this bridge are approximately 74 and 79 percent of the wheel-load factors given in the AASHO specifications for an exterior and an interior stringer.

Steel Stringer Bridge.—By placing two vehicles in their respective lanes and by the use of Figure 25, a maximum value of approximately 56 percent of a unit vehicle is found to be distributed to an exterior stringer in both the positive and negative moment sections. This percentage is equivalent to a wheel-load factor of 1.12. The corresponding wheel-load distribution factors for an interior stringer are found to be approximately 1.33 and 1.40 for the positive and negative moment sections. As in the case of the previous bridge, the maximum experimental wheel-load factors are obtained at sections 2 and 3 for the exterior stringers, and at sections 1 and 4 for the interior stringers. These factors are approximately 78 and 83 percent of the values obtained from the AASHO specifications of 1.44 and 1.638 for the exterior and interior stringers.

CONCLUSIONS

Considerable variation was found to exist in the amount of composite action. The exterior stringers had a larger composite section than the specifications would allow, whereas the interior stringers generally had less.

Composite action did occur at the interior supports even though negative live-load moments cause tension in the concrete roadway slab.

The same type of lateral load distribution occurred for both static and dynamic loading conditions.

Influence lines obtained from the experimental load distribution data yield wheel-load factors which are considerably less than the wheel-load factors obtained by the AASHO specifications for the type of structures studied.

ACKNOWLEDGMENTS

Acknowledgement is due to the Iowa Highway Research Board who sponsored this project. Also, the cooperation and assistance of Mark Morris, Steve Roberts, Neil Weldon, and Carl Schach, all of the Iowa Highway Commission, are especially appreciated.

REFERENCES

1. Caughey, R. A., and Senne, J. H., "Distribution of Loads in Beam and Slab Bridge Floors." Final Rpt., Iowa HRB, Iowa Eng. Exp. Sta., Iowa State Univ. (Sept., 1959).
2. Holcomb, R. M., "Distribution of Loads in Beams and Slab Bridges." Iowa HRB Bull. 12, Ames (1959).
3. Hulsbos, C. L., and Linger, D. A., "Dynamic Tests of a Three-Span Continuous I-Beam Highway Bridge." HRB Bull. 279, pp. 18-46 (1960).
4. Linger, D. A., and Hulsbos, C. L., "Dynamics of Highway Bridges." Joint Publication, Iowa Eng. Exp. Sta., Bull. 188, and Iowa HRB Bull. 17, Ames (1960).
5. Linger, D. A., and Hulsbos, C. L., "Forced Vibration of Continuous Highway Bridges." HRB Bull. 339, pp. 1-22 (1962).
6. Newmark, N. M., "Design of I-Beam Bridges." ASCE Proc. (Mar., 1948).
7. Siess, C.P., and Veletsos, A.S., "Distribution of Loads to Girders in Slab-and-Girder Bridges: Theoretical Analyses and Their Relation to Field Tests." HRB Res. Rpt. 14-B, pp. 58-74 (1952).
8. Wise, J.A., "Dynamics of Highway Bridges." HRB Proc., Vol. 32, pp. 180-187 (1953).